Structural Engineering and Mechanics, Vol. 41, No. 6 (2012) 735-750
DOI: http://dx.doi.org/10.12989/sem.2012.41.6.735

Comparison between two geometrical nonlinear methods for truss analyses

M. Greco*[1], R.C.G. Menin[2a], I.P. Ferreira[1b] and F.B. Barros[1c]

[1]*Graduate Program in Structural Engineering, Department of Structural Engineering, School of Engineering, Federal University of Minas Gerais, Belo Horizonte, Brazil*
[2]*Department of Civil and Environmental Engineering, Faculty of Technology, University of Brasília, Brasília, Brazil*

(Received February 16, 2011, Revised February 3, 2012, Accepted February 21, 2012)

Abstract. This paper presents a comparison between two different procedures to deal with the geometric nonlinear analysis of space trusses, considering its structural stability aspects. The first nonlinear formulation, called positional, uses nodal positions rather than nodal displacements to describe the finite elements kinematics. The strains are computed directly from the proposed position concept, using a Cartesian coordinate system fixed in space. The second formulation, called corotational, is based on the explicit separation between rigid body motion and deformed motion. The numerical examples demonstrate the performances and the convergence of the responses for both analyzed formulations. Two numerical examples were compared, including a lattice beam with postcritical behavior. Despite the two completely different approaches to deal with the geometrical nonlinear problem, the results present good agreement.

Keywords: nonlinear analysis; FEM; space trusses; positional formulation; corotational formulation

1. Introduction

Geometry changes due to the application of external loads are a critical aspect related with the space trusses collapse. As a consequence, the lack of equilibrium induced by the steady state variation becomes an important issue to be evaluated. Another point is the inconsistency between the numerical models and the mechanical behavior of the structure, which can lead to wrong hypothesis regarding the nonlinear phenomenon. The investigations about such issues are still not complete and several models and nonlinear methods have been proposed so far by different authors, e.g., Saka (2007), Saffari *et al*. (2008) and Hrinda (2010). With the same objective, Thai and Kim (2009) preformed an inelastic analysis of space trusses considering both geometrical and material nonlinearities. Recently, Zhou *et al*. (2009) proposed a method for analysis of prestressed space trusses taking into account the influence of the initial imperfections of members with special interest

*Corresponding author, Professor, E-mail: mgreco@dees.ufmg.br
[a]Ph.D., E-mail: renatomenin@gmail.com
[b]Ph.D. Student, E-mail: ivonepassos@dees.ufmg.br
[c]Professor, E-mail: felicio@dees.ufmg.br

in the stability of the structure.

On the other hand, the unstable equilibrium situation does not necessarily represent loss of the strength capacity of the structure. This will mainly depend on the instability nature, i.e., whether it is local or global. A deep understanding about such behavior is essential for the structural design of space trusses. Mathematically, the nonlinear instability analysis is characterized through response bifurcations of nonlinear differential equations that govern the problem.

The nonlinear analysis is of fundamental importance, since the linear analysis is not able to reflect in a satisfactory manner the real behavior of structures in full service or at the collapse. The geometric nonlinearity is characterized by finite strains followed by changes in the stiffness of the structure for a given level of applied load. Thus, the original and the deformed configurations are quite different and the principle of superposition of effects can not be applied. Therefore, the equilibrium equations must be rewritten considering the deformed configuration. A general solution consists of the equilibrium equations linearization; applying an iterative corrective algorithm based on an appropriate convergence criterion.

It is also necessary to adopt a kinematical description in order to map the displacement of the structure in the space through its strain history. Three kinematical descriptions designed to treat the geometrical nonlinear problem are commonly found in the literature: the Eulerian, the Lagrangian and the corotational descriptions. In the Eulerian approach, the motion is performed in terms of the spatial coordinates and it is commonly used in the analysis of fluid mechanics problems in which attention is focused on the motion of the material through a stationary control volume (Bathe 1996). The Lagrangian approach, Fig. 1, describes the kinematics of the deformation in terms of the coordinate system, fixed in space, and three configurations: an original configuration C_0, at a time $t_0 = 0$, a current or intermediate configuration C_1, at a time $t_1 = t + \Delta t$ and a final configuration C_2, at a time $t_2 = t$. In problems involving structural solids using step by step procedures, where the interest is focused in the history of deformation of the body, the Lagrangian description is particularly appropriate. Finally, the corotational approach is based on a explicit separation of the rigid body and the deformed motions (Cook 2001). This separation aims to represent the nonlinearity by the rigid body motions. Therefore, considering some pre-requisites, linear models can be adopted for the finite element description of the deformation history.

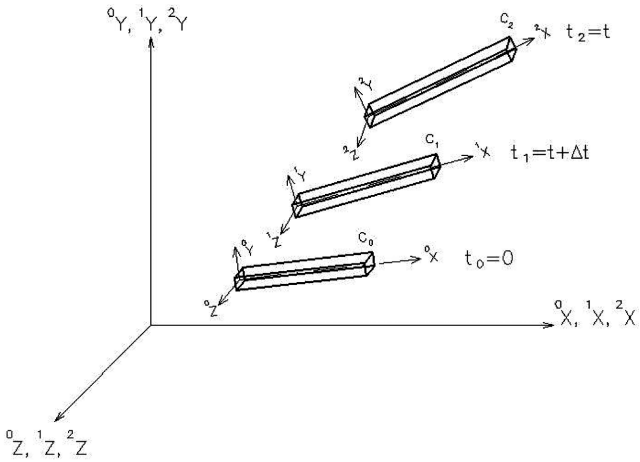

Fig. 1 Lagrangian kinematical description

The specific purpose of this paper is to compare the classical corotational description and a particular case of the Lagrangian formulation, originally presented in Coda and Greco (2004), for reticulated structures under the finite element approach, considering structural stability aspects. These two different numerical formulations will be used here to simulate the geometrical nonlinear behavior of trusses. The positional concept describes the elements kinematics in terms of a global coordinate system, without matrix transformations and strain measure separations. Philosophically, these two formulations are antagonistic. Finally this work aims to prove the invariance of the nonlinear equilibrium for both formulations, whatever the spatial description adopted.

2. Positional formulation

Generally, structural problems are solved by formulations based on equilibrium considerations, such as the Principle of Virtual Work. This is a successful technique for the analysis of trusses undergoing large displacements, before and after the loss of stability (Toklu 2004). The formulation described in this paper, and named positional, is derived from another, but equivalent, approach, i.e., the application of the principle of minimum potential energy. This technique presents a physical sense, instead of a pure mathematical sense. The positional formulation is based on Finite Element Method and it can be classified as a total Lagrangian formulation with exact kinematics. Moreover, instead of displacements, the kinematics of the positional formulation deals with nodal positions. The stiffness matrix is represented by the Hessian matrix and the calculation of the strain follows directly from the proposed concept.

2.1 Formulation

For a conservative structural system, associated with a reference system fixed in space, the principle of minimum potential energy establishes a total potential energy (Π) as follows

$$\Pi = U - \Sigma FX \tag{1}$$

where X is the set of positions independent of each other, which may be occupied by a body material point and F represents the independent applied forces. It is interesting to note that the applied force potential energy may not be zero in the initial configuration. Considering an isotropic, homogeneous and elastic material, governed by a logarithmic strain measure, the structural strain energy (U) can be written for the reference volume V, in a Lagrangian sense.

$$U = \int_V u dV = \int_V \int_{\varepsilon_{\ln}} \sigma_{\ln} d\varepsilon_{\ln} dV \tag{2}$$

where $\varepsilon_{\ln}$ is the logarithmic strain measure and $\sigma_{\ln}$ is its associated stress conjugate. This stress tensor is related with the Cauchy's stress tensor (σ) by the stretching ratio (λ) and the Young's modulus (E), as presented in Greco and Ferreira (2009). The term u represents the specific strain energy.

At this point, the geometry of the studied body should be mapped to know its relation with the adopted strain measurement. Fig. 2 presents the general kinematics for a space truss finite element.

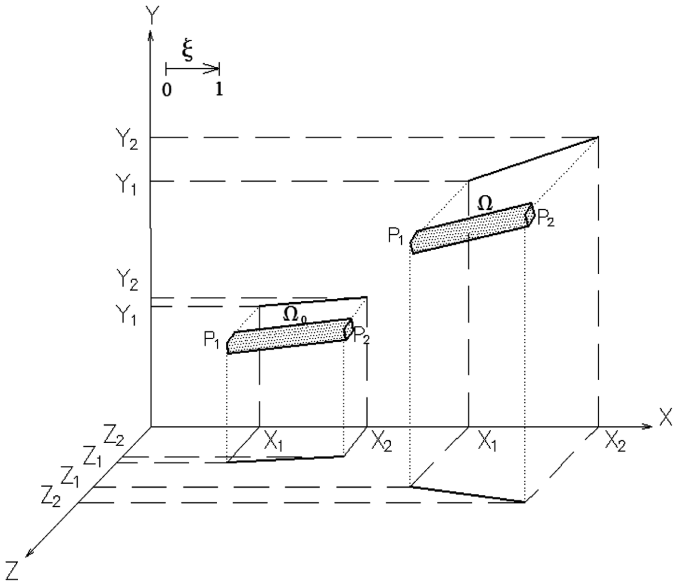

Fig. 2 Space truss finite element at initial configuration (Ω_0) and deformed configuration (Ω)

The truss finite element kinematics shown in Fig. 2 can be parameterized in terms of a dimensionless coordinate ξ (varying from 0 to 1).

$$x = X_1 + (X_2 - X_1)\xi \tag{3}$$

$$y = Y_1 + (Y_2 - Y_1)\xi \tag{4}$$

$$z = Z_1 + (Z_2 - Z_1)\xi \tag{5}$$

The formulation does not involve transformations among systems of local coordinates for global coordinates. Indeed, no local system of coordinates is used in the positional formulation. The nonlinear position formulation used here adopts the stretching ratio concept, defined by the relation between the deformed length (ds) and the initial length (ds_0).

$$\lambda = \frac{ds}{ds_0} = \frac{ds/d\xi}{ds_0/d\xi} \tag{6}$$

The logarithmic strain measure can be used to obtain a geometrically nonlinear formulation that considers materials with large strains.

$$\varepsilon_{\ln} = \ln(\lambda) \tag{7}$$

Thus, the total strain energy can be written in terms of the non-dimensional space, considering constant cross-section area over the finite elements.

$$U = \int_0^l l_0 EA\left(\frac{\lambda^2}{2} - \lambda\right) d\xi = \int_0^l l_0 u d\xi \tag{8}$$

The integral in Eq. (8) along the finite element length (along ξ) yields the exact solution. Since the strain energy is written in terms of nodal positions, the total potential energy can be

differentiated to obtain the equilibrium equation.

An arc-length procedure is adapted to the positional formulation to compare results with the corotational formulation. The arc-length procedure is very suitable for nonlinear responses involving critical points analyses. After the positions or the displacements have reached certain limit, the signs of the prescribed values and the residual vector must be changed. The residual vector is defined by Eq. (9).

$$\frac{\partial \Pi}{\partial X_i} = g(X) = l_0 \int_0^1 \frac{\partial u}{\partial X_i} d\xi - F_i = 0 \tag{9}$$

In order to make easier finding responses after critical points, the decomposition of Bathoz and Dhatt (1979) is used together with the arc-length scheme proposed by Crisfield (1981). It is important to note that, in this study, the applied forces are independent of space. The residual vector $g(X)$ is nonlinear in terms of nodal positions.

3. Corotational formulation

In the corotational formulation (Cook 2001), the reference configuration is built by two parts: one that corresponds to the initial configuration C_o and that is kept fixed throughout the analysis, and another one named corotationed configuration, C_R. This configuration varies from element to element and can be obtained through the displacement of rigid body related to configuration C_0. The coordinate system moves together with the element and the strains are measured with respect to local coordinate system of the configuration C_R.

3.1 Kinematical description

Considering, initially, a finite element of a bar moving itself in the tridimensional space and admit, as an initial hypothesis, that the local axis of the element (x_0^e, y_0^e, z_0^e) in initial configuration C_o coincide with the global, material and spatial coordinate systems, designated by (X, Y, Z) and (x, y, z), respectively. It is also assumed that the origin of the system of the local axis in C_o is situated in half of the original length of the element, designated by L_0. The element bar moves from initial configuration C_0 to current configuration C, whose local axis are designated as (x^e, y^e, z^e). Thus, the corotationed configuration C_R is obtained by the rigid body motion of the configuration C_o. The coordinate system moves together with the element to the configuration C, positioning itself symmetrically with respect to current configuration. It can also be observed in Fig. 3, that the corotationed local axis (x_R^e, y_R^e, z_R^e) coincide with the local axis (x^e, y^e, z^e) in C.

Any point P_0 with coordinates (X, Y, Z) at the initial configuration C_0, moves toward the point P_R with coordinates (x_R, y_R, z_R) at the corotationed configuration C_R. Thus, it moves toward the point P with coordinates (x, y, z) in C. The vector of total displacement $\mathbf{u}$ of the particle, in global coordinates, can be calculated as

$$\mathbf{u} = \mathbf{x} - \mathbf{X} \tag{10}$$

The vector of total displacement consists of two parts: one part related with the displacement of rigid body ($\mathbf{u}_R$) and another part related with the deformational displacement ($\mathbf{u}_D$).

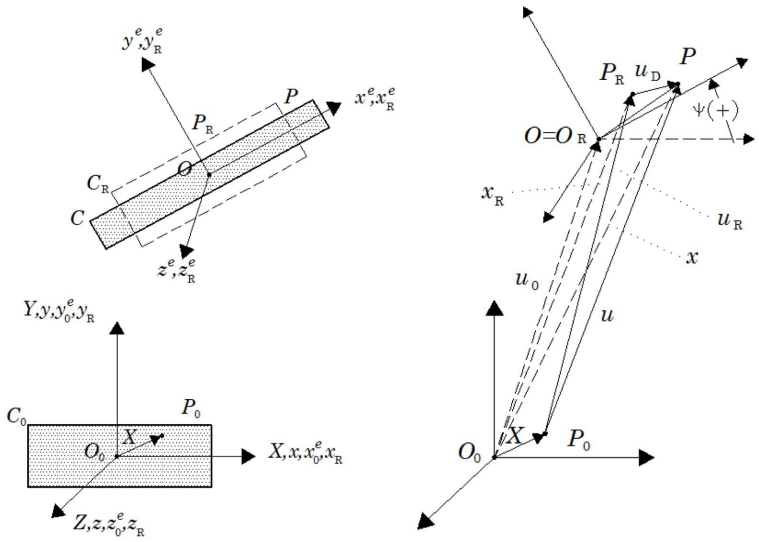

Fig. 3 Bar element in the initial and final configurations

$$\mathbf{u} = \mathbf{u}_R + \mathbf{u}_D = (\mathbf{x}_R - \mathbf{X}) + (\mathbf{x} - \mathbf{x}_R) \tag{11}$$

In the corotational formulation the equations of the deformational movement are written in relation to the local coordinates (x^e, y^e, z^e) at the configuration C, resulting in

$$\mathbf{u}^e_D = \mathbf{R}\mathbf{u}_\mathbf{D} \tag{12}$$

3.2 Coordinate system

The system of the local coordinates (x^e, y^e, z^e) at the current configuration C and at the global configuration (x, y, z) are related to each other by the following expression

$$\mathbf{x}^e = \mathbf{R}(\mathbf{x} - \mathbf{u}_0) \tag{13}$$

The relation expressed in Eq. (13) is illustrated at Fig. 3, being $\mathbf{u}_0$ the vector that represents the displacement from the point O_0 in C_0 to point O in C.

The rotation matrix **R**, that appears in Eqs. (12) and (13), can be defined in term of the co-sine directors (C_x, C_y, C_z) of the bar element at the current configuration C (local axis direction x^e), in relation to the global coordinate system, Fig 4. This matrix, with order 3 for spatial trusses, is used to transform coordinates from the global system (X, Y, Z) to the local system (x^e, y^e, z^e). The deformational displacements $\mathbf{u}^e_D$ are used to obtain the internal force vector and tangent stiffness matrix. It should be noted that it is an orthogonal matrix.

3.3 Deformational displacements

The deformational displacements are obtained in terms of local coordinates, as defined previously

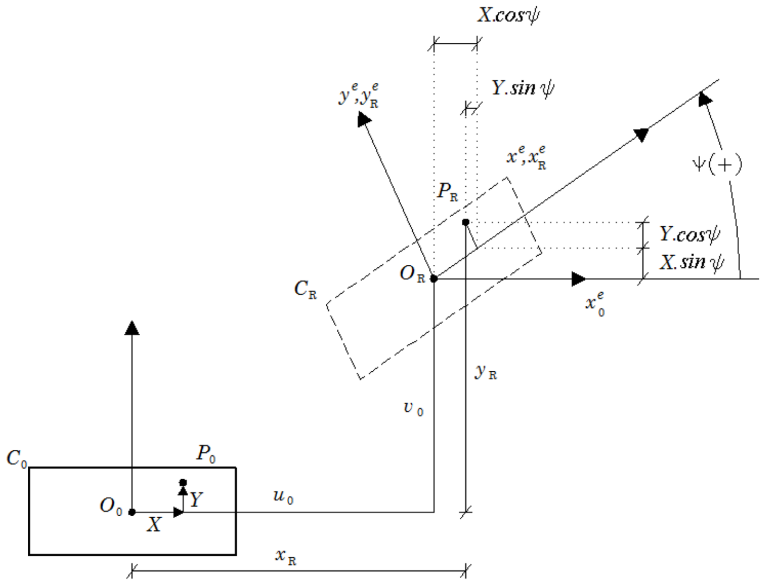

Fig. 4 Position of a particle P_R at the configuration C_R

in Eq. (12). In the case of plane trusses, the coordinate of the particle P_R at configuration C_R can be defined by the following equation

$$\mathbf{x}_R = \begin{Bmatrix} x_R \\ y_R \end{Bmatrix} = \begin{bmatrix} C_x & -C_y \\ C_y & C_x \end{bmatrix} \begin{Bmatrix} X \\ Y \end{Bmatrix} + \begin{Bmatrix} u_0 \\ v_0 \end{Bmatrix} = \mathbf{R}^T\mathbf{X} + \mathbf{u}_0 \tag{14}$$

The coordinates of the particle P at the current configuration C, as shown in Fig. 3, can be expressed by

$$\mathbf{x} = \begin{Bmatrix} x \\ y \end{Bmatrix} = \begin{Bmatrix} X+u \\ Y+v \end{Bmatrix} = \mathbf{X} + \mathbf{u} = \mathbf{I}\mathbf{X} + u \tag{15}$$

Considering the previous equations, one has

$$\mathbf{u}_D = \begin{Bmatrix} u_D \\ v_D \end{Bmatrix} = \begin{Bmatrix} x - x_R \\ y - y_R \end{Bmatrix} = \begin{bmatrix} 1-C_x & C_y \\ -C_y & 1-C_x \end{bmatrix} \begin{Bmatrix} X \\ Y \end{Bmatrix} + \begin{Bmatrix} u-u_0 \\ v-v_0 \end{Bmatrix} = (\mathbf{I} - \mathbf{R}^T)\mathbf{X} + \mathbf{u} - \mathbf{u}_0 \tag{16}$$

Finally, one can obtain the deformational displacement in relation to local coordinates through the transformation of the coordinates, defined in Eq. (12).

$$\mathbf{u}_D^e = \mathbf{R}\mathbf{u}_D = (\mathbf{R} - \mathbf{I})\mathbf{X} + \mathbf{R}(\mathbf{u} - \mathbf{u}_0) \tag{17}$$

In the case of spatial trusses, the coordinates of the particle P_R at the configuration C_R and P at the configuration C are defined analogously to the two-dimensional case.

3.4 Deformational movement as a function of the nodal displacements

The deformational displacements previously defined for a generic point are particularized for the extremity nodes of the bar elements. In the specific case of the plane trusses, the nodal coordinates of the element at the configuration C_0 in relation to local axis are $X_2 = -X_1 = ½ L_0$ and $Y_2 = Y_1 = 0$. Where L_0 is the initial length of the element. The displacements of the extreme nodes can be defined by

$$\mathbf{u} = \begin{Bmatrix} \mathbf{u}_1 \\ \mathbf{u}_2 \end{Bmatrix} = \begin{Bmatrix} u_1 \\ v_1 \\ u_2 \\ v_2 \end{Bmatrix} = \begin{Bmatrix} u(X_1, Y_1) \\ v(X_1, Y_1) \\ u(X_2, Y_2) \\ v(X_2, Y_2) \end{Bmatrix} = \begin{Bmatrix} u\left(\frac{-1}{2L_0}, 0\right) \\ v\left(\frac{-1}{2L_0}, 0\right) \\ u\left(\frac{1}{2L_0}, 0\right) \\ v\left(\frac{1}{2L_0}, 0\right) \end{Bmatrix} \tag{18}$$

Similarly, the deformational movement can be expressed in terms of the nodal displacements. Thus, the Eq. (17) can be equally written in terms of nodal displacements, as follows

$$\mathbf{u}_D^e = \begin{Bmatrix} u_{1D}^e \\ u_{1D}^e \\ u_{2D}^e \\ u_{2D}^e \end{Bmatrix} = \begin{bmatrix} C_x & C_y & 0 & 0 \\ -C_y & C_x & 0 & 0 \\ 0 & 0 & C_x & C_y \\ 0 & 0 & -C_y & C_x \end{bmatrix} \begin{Bmatrix} u_1 - u_0 \\ v_1 - u_0 \\ u_2 - u_0 \\ v_2 - u_0 \end{Bmatrix} + \frac{1}{2} L_0 \begin{Bmatrix} 1 - C_x \\ C_y \\ C_x - 1 \\ -C_y \end{Bmatrix} \tag{19}$$

As the displacement field of the element is linear in X and in Y, the element remains straight at the current configuration C, therefore, it is possible to write

$$u_0 = \frac{1}{2}(u_1 + u_2) \qquad v_0 = \frac{1}{2}(v_1 + v_2) \tag{20}$$

The next step is to define the values of the cosine directors (C_x, C_y) in terms of nodal displacements and then finding the length of the element (L) at the current configuration, as shown in Fig. 5. It is necessary to emphasize that in this deduction, the current configuration has not been aligned with global axis.

Thus, it is necessary to make the rotation of the nodal displacements in terms of system of local axis in the current configuration (x_0^e, y_0^e, z_0^e). Once known the nodal displacements rotated, it is possible to define the other kinematical variables involved in the corotational formulation in terms of the geometric relations.

It is assumed a linear relation between the pars of conjugate stress and strain in the initial and final configurations. Considering this hypothesis and defining the cross section area of the elements at the configurations C_0 e C as being, respectively, A_0 e A, the strain energy of a truss element at the initial and current configurations can be defined by

$$U_0 = \frac{1}{2}\int_0^{L_0} EA_0 \varepsilon_X^2 dX^e \tag{21}$$

Finally, it is necessary to emphasize the importance of choosing the appropriate measurement of strain for the approach of nonlinear problems, as can be seen in Bathe (1996). Depending on the type of analysis different measures of strain can be used. It is possible that the structure undergoes large displacements and small strains. In this case, the initial and final configurations are very similar. So the strains can be infinitesimal, and the measure of strain will not influence the quality of response. On the other hand, the structure can undergo large displacements and deformations. Now the strains must be finite and different strains measures may produce quite different responses to the same structural analysis.

The corotational formulation presented in this paper uses the same logarithmic strain measure used in the positional formulation, shown in Eq. (7).

4. Numerical applications

The following examples compare the numerical results obtained from the positional formulation and from the corotational formulation.

4.1 Two-member plane truss

The first numerical example is a plane truss of two finite elements, as shown in Fig. 5. The dimensions of the structure are given meters. The structure is loaded by a vertical downwards force. The adopted physical and geometric properties are $E = 7.17 \times 10^{10}$ N/m^2 and $A = 0.6 \times 10^{-4}$ m^2.

Fig. 6 shows the response of the structure for several loading levels. It is possible note that, due to its configuration, this structure is very susceptible to reversal of the equilibrium caused by the snap-through phenomenon. The arc-length responses converge, showing the full snap-through curve. It was used an arc-length parameter of 0.05 m (ΔS) for the both nonlinear formulations. The responses of the positional and the corotational implemented formulations are compared with ANSYS® software numerical responses. The commercial software uses the corotational formulation, with arc-

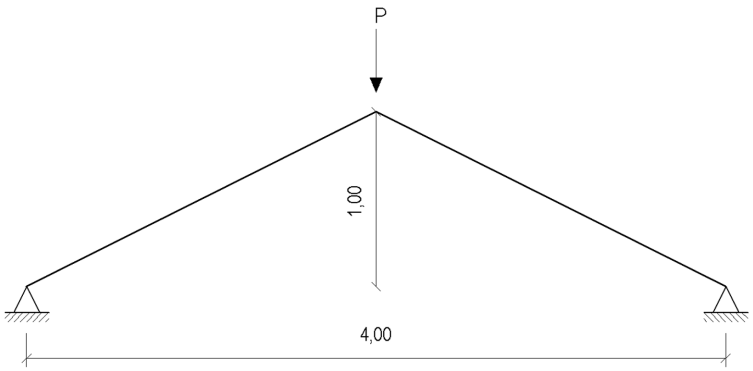

Fig. 5 Two-member plane truss geometry and boundary conditions

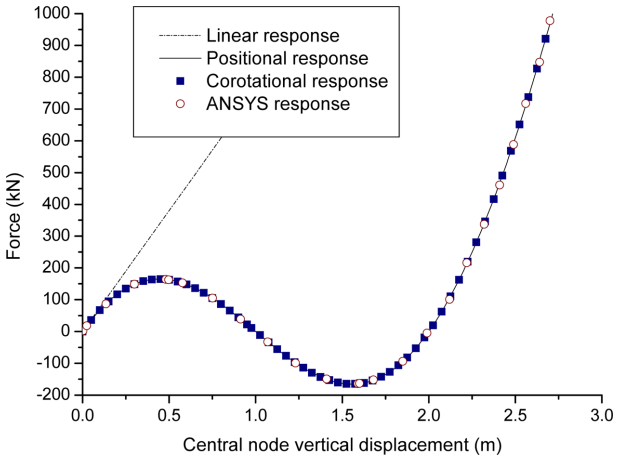

Fig. 6 Force **x** vertical displacement at central node

length procedure, and the logarithmic strain measure for nonlinear analyses. It is also presented the linear response that is valid only at the beginning of the analysis.

For the nonlinear formulations, it was adopted the arc-length procedure presented in the paper of Crisfield (1981) that uses the equation of the circumference, Eq. (22), forcing an equal increment in the arc-length for every iterations of the step.

$$\Delta u \cdot \Delta u = (\Delta S)^2 \tag{22}$$

The results of two implemented formulation and of ANSYS® software were very close, despite the different approaches used to solve the nonlinear equilibrium.

Fig. 7 shows three different configurations of the deformed structure representing important moments in the analysis. At the first configuration, Fig. 7(a), it can be observed a small displacement (7 cm), the structure is close to the initial configuration and therefore it is in the linear regime. At a certain level of loading the structure begins to exhibit behavior essentially nonlinear as shown in Fig. 7(b). The displacement was greater in the second case (30.5 cm) but not enough to the loss of the structural stability. The analysis continues until the load reaches a position that triggers the reversal of the structural behavior due to a larger displacement (2.25 m). Thus, the structural members that were initially compressed, to reach the new equilibrium configuration, are now fully tensioned, as shown in Fig. 7(c).

It should be noted that, for both formulations, positional and corotational, the iterative steps were evaluated with only two iterations during the nonlinear equilibrium solutions. Oscillations of the arc-length response may occur at critical points, when the gradient of the strain energy and the Laplacian of the strain energy are singular (Greco and Venturini 2006). In this case, the critical point is a limit point, instead of a bifurcation point. The equilibrium was obtained due to the adopted maximum number of iteration, i.e., fifty iterations. The adopted arc-length parameter is equal to the maximum arc-length ($\Delta S = \Delta S$ max = 0.05 m) and the adopted minimum arc-length is equal to 0.005 m.

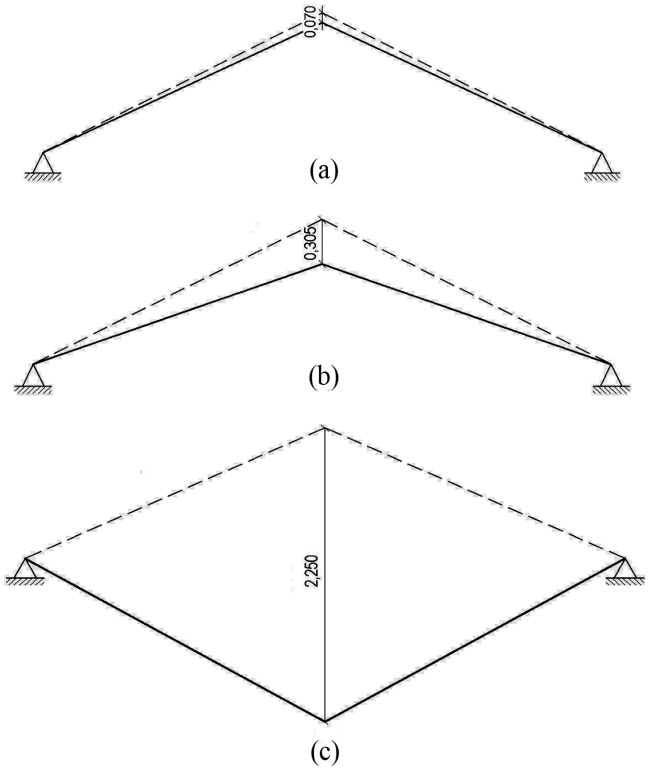

Fig. 7 Deformed configurations of the structure

4.2 Lattice beam

The structure of this example, which can be found originally in Noor and Peters (1980), consists of 28 nodes and 76 bars with the dimensions given in Fig. 8, with units in meters. The response comparison among the considered formulations and ANSYS® response regards to the vertical displacements of the node number 10. The physical and geometric properties are given as follows:

Cross-sectional area of the longitudinal members = 0.8×10^{-4} m^2
Cross-sectional area of the transversal members = 0.6×10^{-4} m^2
Cross-sectional area of the diagonal members = 0.4×10^{-4} m^2
$E = 7.17 \times 10^{10}$ N/m^2 (Young's modulus)

It was also used an arc-length parameter of 0.05 m (ΔS) for the both nonlinear formulations. The structure is analyzed for two different boundary conditions, with or without lateral bracing. For the case with lateral bracing, it is assumed that all nodes in the direction of the Z coordinate will be supported. The fundamental solution, presented in Fig. 9 was obtained for the case lateral bracing. On the other hand, no lateral support is considered for the secondary path. The analyses were performed by the corotational and positional formulations.

It can be observed in Fig. 9 that both implemented formulations have practically presented the same results. The ANSYS® solution was close to the other solutions up to the limit point. Afterwards, the ANSYS® response presented slightly crescent numerical divergences from the other

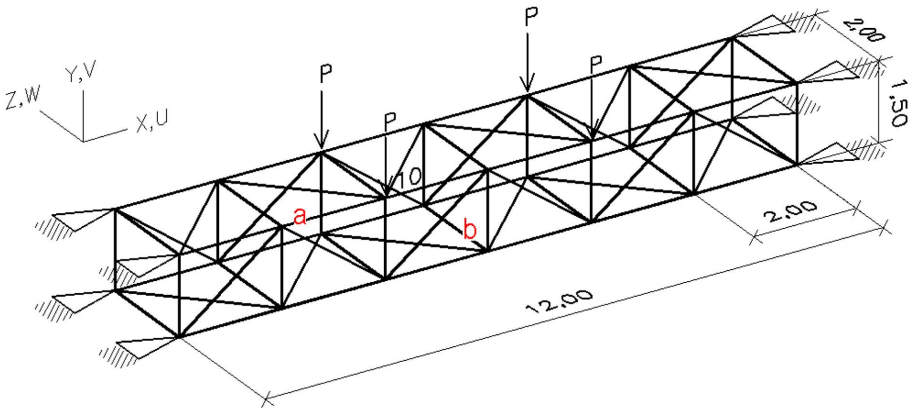

Fig. 8 Lattice beam geometry and boundary conditions

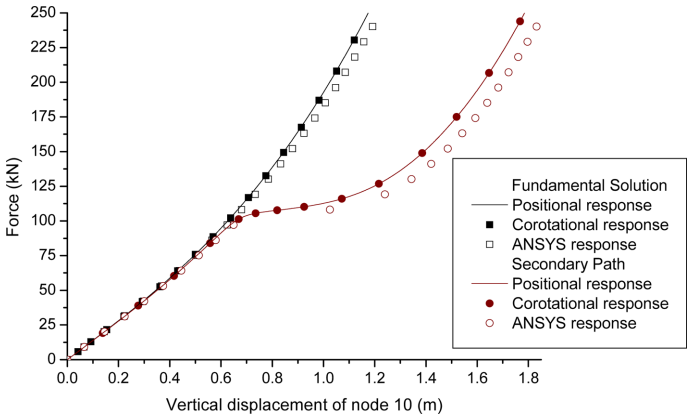

Fig. 9 Positional **x** Corotational, with displacements observed at node 10

numerical responses. At the vicinity of force 100 kN it is observed a critical point related with a response bifurcation. It also can be observed that the bracing at the *Z* direction decreases the global structural stiffness. The fundamental solution is associated with the first limit point, while the secondary solution is associated with a buckling phenomenon. The buckling occurs before the limit point which is assumed as the limit load for practical applications. In Fig. 10, for the case without lateral bracing, it is observed only one change of slope after a maximum value is achieved. On the other hand, for lateral bracing, Fig. 11, there is a considerable reduction of the effort and it is observed two changes of slope. Both of the illustrated cases refer to traction efforts.

In Fig. 12, for the case without lateral bracing, it is possible to note the reversal of efforts in the longitudinal element (b), starting as compressive forces and ending as traction ones. For the case with lateral bracing, Fig. 13, this is not observed anymore and there is a substantial increase of the traction effort. Such different behavior can be explained by the redistribution of the efforts caused by the existence of the lateral bracing.

Figs. 14 to 17 present the deformed configurations of the lattice beam, obtained from the

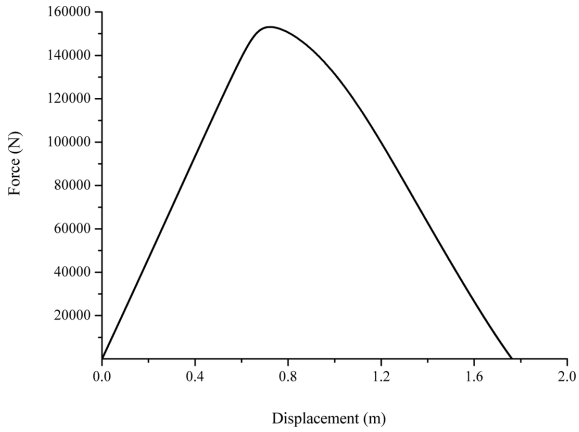

Fig. 10 Normal forces in the longitudinal element (a) without brancing

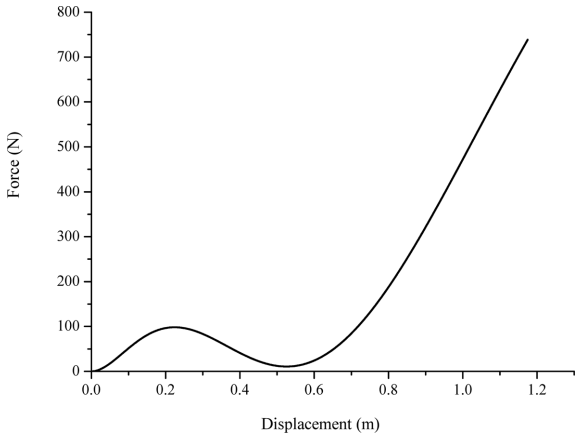

Fig. 11 Normal forces in the longitudinal element (a) with brancing

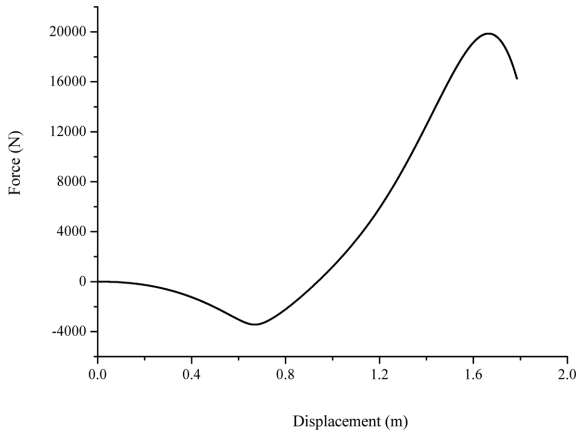

Fig. 12 Normal forces in the transversal element (b) without brancing

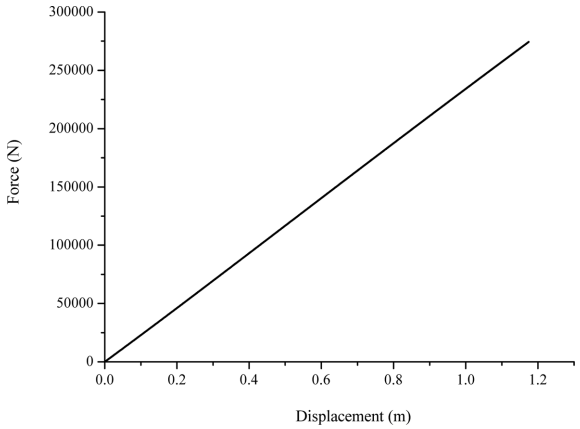

Fig. 13 Normal forces in the transversal element (b) with brancing

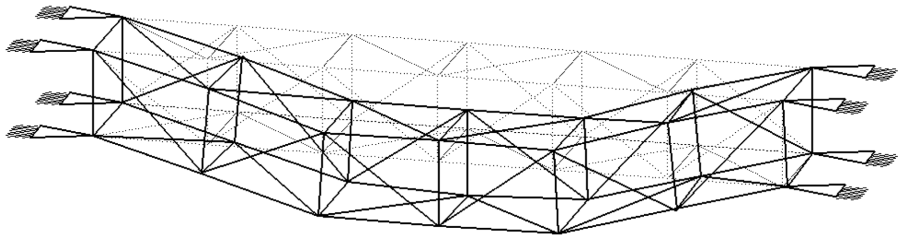

Fig. 14 Perspective of the deformed structure (fundamental solution)

positional formulation, for the ultimate applied force of the analysis (250 kN). It is possible to observe the buckling effects in the secondary solution.

Figs. 18 and 19 present the normalized residues at four vertical positions of node 10, in logarithmic scale, obtained from the positional and from the corotational formulations. These figures

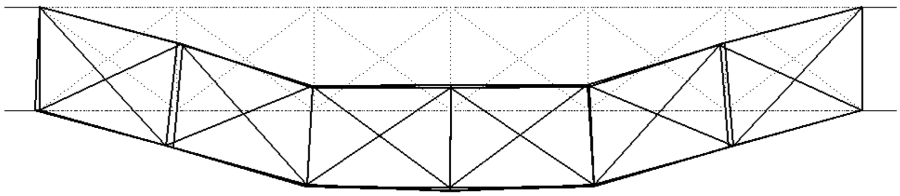

Fig. 15 Lateral view of the deformed structure (fundamental solution)

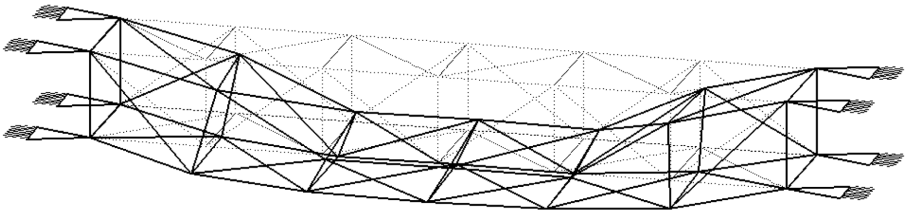

Fig. 16 Perspective of the deformed structure (secondary solution)

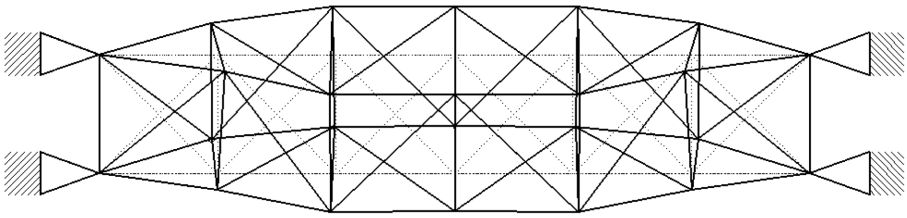

Fig. 17 Inferior view of the deformed structure (secondary solution)

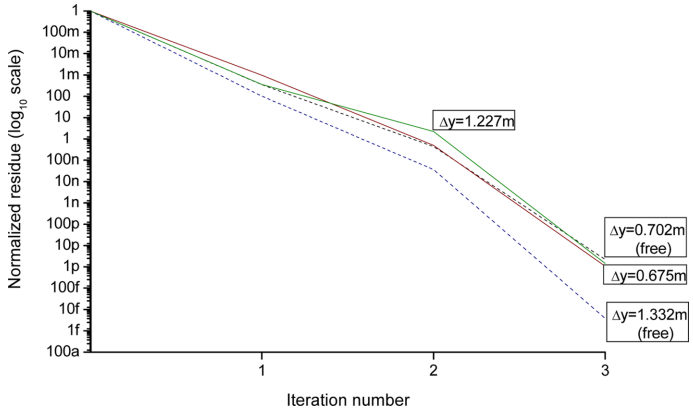

Fig. 18 Normalized residues at four vertical positions of node 10, obtained from the positional formulation

point to the high accuracy of the formulations, both working with quadratic rate of convergence due to the full Newton-Raphson procedure used. In these figures, the free caption refers to the secondary solution (not supported in the Z direction). The corotational formulation presents less iteration than the positional formulation. Nonetheless, at critical points the positional formulation presents better reliability for the numerical calculation.

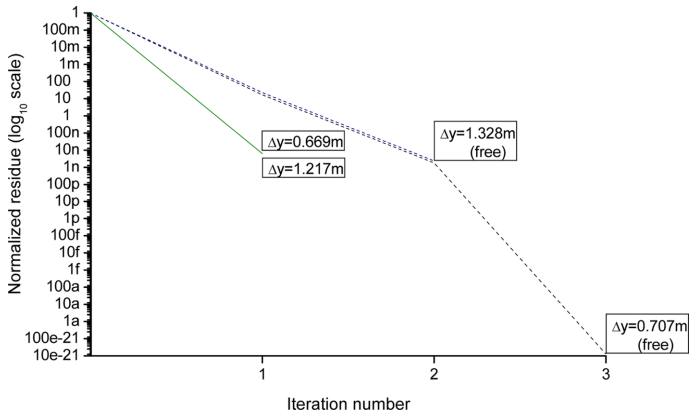

Fig. 19 Normalized residues at four vertical positions of node 10, obtained from the corotational formulation

5. Conclusions

Two nonlinear formulations were algebraically developed and implemented, using FORTRAN codes, and its numerical performances were compared with ANSYS® software numerical responses. The relatively new positional formulation, combined with its computational implementation, has shown satisfactory results when compared to the classical corotational formulation. Two numerical examples were analyzed, representing a plane and a spatial truss with severe nonlinear geometric behavior. For both examples, there were no notable differences between the results of the formulations. The ANSYS® numerical responses present differences after the limit point of the lattice beam numerical example. In general terms, the positional formulation is considerable simpler than the corotational formulation. Thus, the numerical evaluation performed by the positional formulation can be potentially faster than the numerical evaluation performed by the corotational formulation**,** due to its simplicity, being very appropriate for complex structural analysis with high dimension matrix operations. On the other hand, in the case of the corotational formulation, the reuse of the computational code for other materials constitutive laws formulations is an evident advantage. To derive a numerical formulation for new materials or phenomena using the positional concept, the new terms must be included at the initial functional of energy, leading to a considerable amount of algebraic deployment.

Acknowledgments

This work was supported in part by the CNPq (National Council of Scientific and Technological Development) under grant numbers 571319/2008-4, 305626/2010-8 and 301487/2010-3.The authors would like to acknowledge FAPEMIG (Minas Gerais State Research Foundation) for financial support under grants numbers TEC - PPM-00139-09 and TEC-PPM-00201-10. Finally, the authors would also like to thank Ronaldo Romão da Silva for the CAD figures.

References

Bathe, K.J. (1996), *Finite Element Procedures*, Prentice Hall Inc., New Jersey.

Batoz, J.L. and Dhatt, G. (1979), "Incremental displacement algorithms for non-linear problems", *Int. J. Numer. Meth. Eng.,* **14**, 1262-1266.

Coda, H. and Greco, M. (2004), "A simple FEM formulation for large deflection 2D frame analysis based on position description", *Comput. Meth. Appl. Mech. Eng.*, **193**, 3541-3557.

Cook, R.D. (2001), *Concepts and Applications of Finite Element Analysis*, 3rd Edition, John Wiley & Sons Inc., New York.

Crisfield, M.A. (1981), "A fast incremental-iterative solution procedure that handles snap-through", *Comput. Struct.*, **13**, 55-62.

Greco, M. and Venturini, W.S. (2006), "Stability analysis of three-dimensional trusses", *Latin Am. J. Solids Struct.*, **3**, 325-344.

Greco, M. and Ferreira, I.P. (2009), "The logarithmic strain measure applied to the nonlinear positional formulation for space truss analysis", *Finite Elem. Analy. D.*, **45**, 632-639.

Hrinda, G.A. (2010), "Snap-through instability patterns in truss structures", Nasa Langley Research Center, Hamptom, Virginia, 23831.

Noor, A.K. and Peters, J.M. (1980), "Nonlinear dynamic analysis of space trusses", *Comput. Meth. Appl. Mech. Eng.*, **21**, 1311-151.

Saffari, H., Fadaee, M.J. and Tabatabaei, R. (2008), "Nonlinear analysis of space trusses using modified normal flow algorithm", *J. Struct. Eng.*, **134**, 998-1005.

Saka, M.P. (2007), "Optimum topological design of geometrically nonlinear single layer latticed domes using coupled genetic algorithm", *Int. J. Space Struct.*, **85**, 1635-1646.

Thai, H.T. and Kim, S.E. (2009), "Large deflection inelastic analysis of space trusses using generalized displacement control method", *J. Constr. Steel Res.*, **65**, 1987-1994.

Toklu, Y.C. (2004), "Nonlinear analysis of trusses through energy minimization", *Comput. Struct.*, **82**, 1581-1589.

Zhou, Z., Meng, S.P. and Wu, J. (2009), "Stability analysis of prestressed space truss structures based on the imperfect truss element", *Int. J. Steel Struct.*, **9**(3), 253-260.